Invasion patterns in brain metastases of solid cancers

Berghoff, A S ; Rajky, O ; Winkler, F ; Bartsch, R ; Furtner, J ; Hainfellner, J A ; Goodman, S L ; Weller, M ; Schittenhelm, J ; Preusser, M

Abstract: Background Brain metastases are generally considered to be well demarcated from the surrounding brain parenchyma, although infiltrative growth patterns have been observed. We systemically investigated infiltration patterns and expression of adhesion molecules in a large and well-defined series of autopsy cases of brain metastases. Methods Ninety-seven autopsy specimens from 57 brain metastasis patients (primary tumor: 27 lung cancer, 6 breast cancer, 8 melanoma, 2 colorectal cancer, 1 kidney cancer, and 13 other) were evaluated for patterns of invasion into surrounding brain parenchyma. Expression of integrins v; cytoplasmic 3, v 3, v 5, v 6, and v 8; and of E and N cadherin were evaluated using immunohistochemistry. Results Three main invasion patterns were seen: well-demarcated growth (29/57, 51%), vascular co-option (10/57, 18%), and diffuse infiltration (18/57, 32%). There was no statistically significant association of invasion pattern with primary tumor type, although vascular co-option was most common in melanoma brain metastases (4/10). Invasion patterns of different brain metastases of the same patient were highly concordant ($P < .001$, chi-square test). Distance of infiltration from the main tumor mass ranged from 12.5 µm to 450 µm (median 56.2 µm) and was not significantly different between the vascular co-option and the diffuse infiltration groups. Levels of v 6 were significantly higher in the well-demarcated group than in the vascular co-option and the diffuse infiltration groups ($P = .033$, Kruskal-Wallis test). Expression of v 5 in tumor cells was higher in brain metastasis lesions previously treated with stereotactic radiosurgery ($P = .034$, chi-square test). Conclusions Distinct invasion patterns of brain metastases into the brain parenchyma are not specific for primary tumor types, seem to be influenced by expression of v integrin complexes, and may help to guide clinical decision-making.

DOI: https://doi.org/10.1093/neuonc/not112

INVASION PATTERNS IN BRAIN METASTASES OF SOLID CANCERS

Anna S. Berghoff[1,3], Orsolya Rajky[2,3], Frank Winkler[4], Rupert Bartsch[2,3], Julia Furtner[5], Johannes A. Hainfellner[1,3], Simon L. Goodman[6], Michael Weller[7], Jens Schittenhelm[8], Matthias Preusser[2,3]

1 Institute of Neurology, Medical University of Vienna, Vienna, Währinger Gürtel 18-20, 1090 Vienna, Austria

2 Department of Medicine I, Medical University of Vienna, Vienna, Währinger Gürtel 18-20, 1090 Vienna,Austria

3 Comprehensive Cancer Center – CNS Unit (CCC-CNS), Vienna, Währinger Gürtel 18-20, 1090 Vienna,Austria

4 Neurology Clinic and National Center for Tumor Disease, University of Heidelberg, Im Neuenheimer Feld, 400 69120 Heidelberg, Germany

5 Department of Radiology, Medical University of Vienna, Vienna, Währinger Gürtel 18-20, 1090 Vienna, Austria

6 Therapeutic Area Oncology, Cellular Pharmacology, Merck-Serono, Merck KGaA, 64293 Darmstadt, Germany

7 Department of Neurology, University Hospital Zurich, Frauenklinikstrasse 26 8091 Zurich , Switzerland

8 Department of Neuropathology, Institute of Pathology and Neuropathology, University of Tübingen, Liebermeisterstraße 8, 72076 Tübingen, Germany.

CORRESPONDING AUTHOR:

Matthias Preusser, MD

Department of Medicine I and Comprehensive Cancer Center

Central Nervous System Tumours Unit (CCC-CNS)

Medical University of Vienna,

Waehringer Guertel 18-20 ,1090 Vienna, Austria

Tel: 00431-40400-4457, Fax: 00431-40400-6088

E-mail: matthias.preusser@meduniwien.ac.at

FUNDING

The costs for this project were covered by the research budget of the Medical University of Vienna and the University of Tübingen.

CONFLICT OF INTEREST

SLG is employee at Merck-Serono and has a patent application referring to the anti-integrin antibodies used here. MW has received research support and honoraria for lectures and advisory board from Merck-Serono. All other authors declare no conflict of interest.

ABSTRACT

Background: Brain metastases are generally considered to be well-demarcated from the surrounding brain parenchyma, although infiltrative growth patterns have been observed. We systemically investigated infiltration patterns and expression of adhesion molecules in a large and well-defined series of autopsy cases of brain metastases.

Methods: 97 autopsy specimens from 57 brain metastases patients (primary tumor: 27 lung cancer, 6 breast cancer, 8 melanoma, 1 kidney cancer, 2 colorectal cancer, 13 other) were evaluated for the patterns of invasion into surrounding brain parenchyma. Expression of integrins αv, cytoplasmic β3, αvβ3, αvβ5, αvβ6 and αvβ8, and of E and N cadherin were evaluated using immunohistochemistry.

Results: Three main invasion patterns were seen: well-demarcated growth (29/57, 51%), vascular co-option (10/57, 18%) and diffuse infiltration (18/57, 32%). There was no statistically significant association of invasion pattern with primary tumor type, although vascular co-option was most common in melanoma brain metastases (4/10). Invasion patterns of different brain metastases of the same patient were highly concordant ($p<0.001$; Chi Square test). Distance of infiltration from the main tumor mass ranged from 12.5 µm to 450 µm (median 56.2 µm) and was not significantly different between the vascular co-option and the diffuse infiltration groups. αvβ6 levels were significantly higher in the well-demarcated group than in the vascular co-option and the diffuse infiltration groups ($p=0.033$; Kruskal-Wallis

test), respectively. αvβ5 expression in tumor cells was higher in brain metastases lesions previously treated with stereotactic radiosurgery (p=0.034; Chi square test).

Conclusions: Distinct invasion patterns of brain metastases into the brain parenchyma are not specific for primary tumor types, seem to be influenced by expression of αv integrin complexes and may help to guide clinical decision making.

Keywords: brain metastases, invasion, adhesion molecules, integrine, cadherine

INTRODUCTION

Brain metastases are a frequent complication in oncology and affect up to 40% of patients with metastatic cancer. [1] While the incidence of brain metastases showed a constant increase over the last decades, treatment options remain limited and rely mainly on local approaches like surgery, radiosurgery, or whole brain radiotherapy (WBRT). [2-4] Better understanding of the pathobiology of brain metastases may lead to novel treatments.

Brain metastases are usually regarded as growing in a well-delineated fashion within the brain parenchyma. [5] This notion is mainly based on their neuroradiological presentation with relatively sharp demarcation of contrast-enhancing areas and a generally better delineation than that of malignant gliomas. However, the histological patterns of invasion in brain metastases have so far not been addressed in comprehensive studies, although infiltrative behavior has occasionally been noted. [6,7] Clinically, infiltrative behavior with unclear resection margins is regularly noted by neurosurgeons and high local recurrence rates after (radio)-surgery have been reported for such cases. [8,9]

In general, cancer cells grow and invade solid tissues in different ways such as: expansive growth; multicellular migration; or individual cell migration. [10] Migration and invasion require complex regulation of specific molecules including adhesion molecules (e.g. integrins, cadherins), cytoskeletal components (e.g. actomyosin) and proteolytic enzymes (e.g. matrix metalloproteases, MMP) and others. [10-13] However, the types of invasive behavior of tumor cells have been mostly described in models of non-CNS tissues (e.g. skin) and it is unknown whether similar mechanisms are active in the brain, with its distinct microenvironment. The CNS microenvironment

differs from that of other solid organs. The brain parenchmya is composed of highly specialized cells (neurons, astrocytes, oligodendrocytes, microglia) and its extra-cellular matrix (ECM) has a distinct composition. It lacks constituents usually found in solid organs such as fibronectin and collagen, but it is rich in proteoglycans, tenascin, laminin, heparin/chondroitin/dermatan sulfates and hyaluronic acid. [14]

In this study we systemically characterized the invasion patterns of brain metastases and their correlation with the expression of several adhesion molecules in a series of autopsy specimens. Surgery specimens are not suitable for such studies since in most cases they include no or only little well-preserved brain tissue around the resection margin and are thus not sufficient for investigation of the invasion front and the interaction of cancer cells with the brain parenchyma.

METHODS

Patients

All patients with histologically proven brain metastases who underwent brain autopsy between 1987 and 2011 were identified from the Neuro-Biobank of the Medical University of Vienna. Of each patient at least one representative formalin-fixed and paraffin-embedded tissue block containing tumor tissue and surrounding brain parenchyma was selected. Clinical and demographic data were retrieved by chart review. This study was approved by the ethics committee of the Medical University of Vienna (Ethics committee protocol number 078/2004).

Evaluation of invasion patterns

Evaluation of invasion patterns was performed on one routinely stained hematoxylin and eosin (H&E) section per tumor block. For enhanced visibility and better evaluation of single tumor cells, immunohistochemistry for cytokeratin (carcinomas) or HMGB45 (melanomas) and for evaluation of vascular structures immunohistochemistry for CD34 was performed on an automated horizontal slide-processing system (AutostainerPlusLink, Dako, Glostrup, Denmark) using standard protocols in selected cases (**Table 1**). [15-17] Maximal invasion distance of tumor cells from the main tumor mass was microscopically measured on H&E slides with a grid of 25 µm length at 400x magnification.

Immunohistochemistry and evaluation of integrins and cadherins

Immunohistochemistry for αv subunit, cytoplasmic β3, and αvβ3, αvβ5, αvβ6 and αvβ8 complexes was performed with fully-automated multi-modal slide-staining system (BenchMark, Ventana Medical Systems, Strasbourg, France) as described previously. [18] In brief, an indirect biotin-avidin system with standard cell conditioner 1 and EDTA pretreatment protocol were used. Signal amplification was achieved with a copper enhancer (iView DAB Detection Kit; Ventana Medical Systems). [19] Immunohistochemistry for E cadherin and N cadherin was performed using an automated horizontal slide-processing system (AutostainerPlusLink/ Dako). In brief, antigen retrieval was performed with ph9 buffer (Flex TRS high, Dako). Slides were incubated with primary antibody for 1 h for N cadherin (Anti-N cadherin antibody, ab18203, abcam, Cambrige, UK, solution 1:500) and over night for E cadherin (Anti-E cadherin antibody, ab15148, abcam, solution 1:30). Adequate positive and negative controls were included in each run. **Table 1** lists antibodies, clones, dilution, positive controls and sources of reagents.

Analyses of immunohistochemical staining of integrin αv subunit, cytoplasmic β3, αvβ3, αvβ5, αvβ6, αvβ8 complexes, and of E cadherin and N cadherin were performed by calculating the H-score. [20,21] In brief, intensity of membranous staining was multiplied by the percentage of cells showing a specific, complete, membranous immunoreactivity. Further, integrin and cadherin expression of the vascular structures of the surrounding brain parenchyma, tumor vessels, peritumoral vessel and stroma was evaluated semi-quantitatively and recorded as either positive or negative.

Macroscopic autopsy and radiology

For illustrative purposes, we retrospectively retrieved digitalized photographs of the macroscopic autopsy specimens and pre-mortem cranial MR images of the investigated patient cohort from the archives of our Neuro-Biobank and the Department of Neuroradiology where available.

Statistics

We performed exploratory analyses of correlation between invasion pattern and integrin and cadherin expression. For correlation of two binary variables Chi Square test was used. For correlation of median between invasion groups Kruskal Wallis test was performed. For correlation of invasion patterns with time from first diagnosis of brain metastases to death (overall survival time) we used the Kaplan-Meier method and the log-rank test. Patients, in whom brain metastases were detected at death were excluded from survival analysis. As the purpose of the study was exploratory, no adjustment for multiple testing was applied. [22] All statistics were calculated using statistical package for the social sciences (SPSS®) 20.0 software (SPSS Inc., Chicago, IL, USA).

RESULTS

Patients' characteristics

57 patients (26 female, 31 male) with a median age of 58 years (range 27-91) at death were included in the analysis. Overall 97 autopsy specimens were evaluated.. In all 57 patients one brain metastasis tissue block, in 30/57 (52.6%) patients tissue blocks of two distinct brain metastases and in 10/57 (17.5%) patients three tissue blocks of distinct brain metastases were available for investigation. In 18/57 (31.6%) patients diagnosis of brain metastases was made only at autopsy. 23/57 (40.4%) received treatment for brain metastases. First line treatment for brain metastases was surgery in 7/57 (12.3%) patients, stereotactic radiosurgery (SRS) in 8/57 (14.0%), whole brain radiation therapy (WBRT) in 4/57 (7.0%) and chemotherapy in 4/57 (7.0%) patients. Overall 7/57 (12.3%) of patients received WBRT during the course of disease, 7/57 (12.3%) received SRS of the brain metastasis investigated in this study and 17/57 (29.8%) patients received chemotherapy during the course of disease. 34/57 (59.6%) patients were treated with best supportive care upon diagnosis of brain metastases. According to autopsy protocols, brain metastases were the cause of death in 19/57 (33.3%) patients. **Table 2** summarizes further patients' characteristics and detailed compilation is given in supplemental Table 1.

Invasion patterns of brain metastases

Histomorphology

We delineated three distinct invasion patterns: 29/57 (50.9%) brain metastases showed a distinct, well-demarcated border to the surrounding brain parenchyma (well-demarcated group); 10/57 (17.5%; **Figure 1A**) brain metastases showed

distinct perivascular protrusions of multicellular tumor cell formations from the main tumor mass into the brain parenchyma (vascular co-option group, **Figure 1B**); 18/57 (31.6%) brain metastases showed a diffuse infiltration of single tumor cells into the surrounding brain parenchyma (diffuse infiltration group; **Figure 1C**). Generally, the invasion pattern was consistent throughout major parts (>90% of the boarder) of the tumor/brain border in individual metastases.

In 30/57 (52.6%) cases, multiple distinct brain metastases of the same patient were available for investigation and the invasion type was in general highly congruent among the lesions ($p<0.001$ Chi Square test; **Table 3**).

Median maximal measurable invasion distance of tumor cells from the border of the main tumor mass was 68.7 µm (range 12.5-125 µm) in the vascular co-option group and 56.2 µm (range 12.5 – 450 µm) in the diffuse infiltration group. The maximal measurable invasion distance was not different between the vascular co-option group and the diffuse infiltration group ($p=0.486$; t-test).

Correlation with primary tumor type

Brain metastases of melanoma tended to grow via vascular co-option more often than other primary tumors (4/8). The most frequent primary tumor in the well-demarcated as well as in the diffuse infiltration group was lung cancer. Brain metastases of SCLC showed frequently a diffusely infiltrative growth (2/3), while NSCLC grew rather well-demarcated (13/24; 54.2%). Squamous NSCLC were more common in the well-demarcated group (4/6), while adenocarcinoma NSCLC was equally represented in the well-demarcated (5/12; 41.7%) and the diffuse infiltration group (5/12; 41.7%). See **Table 2** for correlation of invasion patterns with primary tumor type.

Correlation with treatment

Complete information on applied therapies after diagnosis of brain metastases was available for 55/57 (96.5%) patients. No statistically significant association was observed between first-line or any-line brain metastases treatment and invasion patterns (**Table 2**). In the diffuse infiltration group a higher proportion of patients had received WBRT at any time point (4/18; 22%) compared to the well-demarcated group (2/28; 7.1%) or the vascular co-option group (1/10). Further, a higher proportion of patients had received chemotherapy during their course of disease in the diffuse infiltration group (8/17; 47.1%) than in the well-demarcated (8/28; 28.6%) or the vascular co-option group (1/10).

Correlation with clinical characteristics

Survival times from first diagnosis of brain metastases were available in 37 patients. Median survival from diagnosis of brain metastases was 2.0 months in the well-demarcated group (n=19), 1.8 months in the vascular co-option group (n= 5) and 1.8 months in the diffuse infiltration group (n= 13). There was no statistically significant correlation of invasion pattern with survival time from diagnosis of brain metastases in this small cohort (p=0.945, log rank test). Patients in the well-demarcated group had more often a singular brain metastases at first diagnosis of brain metastases (52%) than the vascular co-option (33.3%) or diffuse infiltration group (35.7%; p=0.483, Chi square test). Extracranial metastases were present in 19/57 (33.3%) patients. No difference in the presence of extracranial metastases was observed between the three invasion patterns (p=0.781; Chi square test). In the cohort of all 56 patients, there was no significant association of invasion pattern with survival time

(p= 0.825, log-rank test). Correlation with macroscopic pathology findings and neuroradiology

Illustrative correlations of macroscopic pathology and neuroradiological findings with histological invasion patterns are shown in **Figure 1**. The low number of available macroscopic photographs (n=4) and pre-mortal neuroradiological images (n=5) precluded systematic correlation with histological findings.

Integrin expression

General description

av integrins showed strong membranous expression on tumor, vascular, and stromal cells in variable fractions of cases. In general, the majority of specimens showed with homogenous av integrin expression patterns throughout the tumor tissue, except for αvβ8 expression, which was absent in the majority of specimens (supplemental Table 1). However, regional accentuation of integrin expression was observed in some specimens. Accentuated expression in perivascular tumor cells was observed in 11/57 (19.3%), 9/57 (15.8%) and 4/57 (7.0%) for αv subunit, αvβ6 and αvβ5, respectively. Peri-necrotic overexpression of αvβ6, αv subunit and αvβ5 was found in 4/57 (7.0%), 2/57 (3.5%) and 2/57 (3.5%) cases, respectively (**Figure 2**).

Analyzing expression on vascular structures, we observed αvβ5 integrin expression on all (57/57, 100%) vessels including tumoral and peritumoral vessels as well as the vascular structures of the surrounding brain parenchyma. αvβ3 expression was not observed on the vascular structures of the surrounding brain parenchyma, except randomly on some larger vessels of the meninges. Prominent expression of αvβ3 was observed on angiogenic, sprouting vessels with multi-layered endothelium within

the tumor and in the peritumoral area. In 30/57 (52.6%) specimens, immunoreactivity for αvβ3 of the angiogenic tumor vessels was observed and in 29/57 (50.9%) specimens, angiogenic vessels in the peritumoral area showed specific immunoreactivity for αvβ3. Specific immunoreactivity for β3 subunit was observed in angiogenic tumor vessels of 46/57 (80.7%) specimens and in angiogenic vessels in the peritumoral area of 45/57 (78.9%) specimens (**Figure 3**). The expression detected for the αvβ3 complex was generally lower than for the β3 cytoplasmic domain. The β3 chain is on two integrin complexes, αvβ3 and gpiibiiia (the platelet fibrinogen receptor). The tissue localization suggested that the staining of β3 was not due to platelet deposits or aggregates. The αvβ3-antibody used (EM22703) binds preferentially particular ligated conformation of αvβ3, while the cytoplasmic-β3 antibody (EM00212) does not discriminate [18]. This may explain the difference in staining results between these antibodies.

Fibrous tumoral stroma was observed in 32/57 (56.1%) specimens and showed expression of αv subunit (32/32, 100%), αvβ3 (2/32, 6.3%), αvβ5 (28/32, 87.5%) and αvβ6 (6/32, 18.8%).

Relative overexpression of αv integrins at the invasion front was not consistently found, but only in some specimens (αv subunit: 8/57, 14.0%: αvβ5: 8/57, 14.0%; αvβ6: 8/57, 14.0%).

Correlation with invasion patterns

Median H-score of αvβ6 was significantly higher in the well-demarcated (median 90; range 0-300) than in the vascular co-option (median 0; range 0-120) and the diffuse infiltration group (median 30; range 0-120; p=0.033; Kruskal Wallis test). No

correlation of invasion pattern and median H-score of αv subunit, αvβ3, αvβ5, αvβ8 or β3 subunit was observed.

Correlation with therapy

Brain metastases previously treated with stereotactic radiosurgery presented more frequently with αvβ5 expression in the tumor cells (6/7) than specimens without prior stereotactic radiosurgery (21/49, 42.9%; p=0.034; Chi square test). Furthermore, median αvβ5 H-score was significantly higher in brain metastases with prior stereotactic radiosurgery (60 vs. 0; p=0.05, Mann Whitney U test). No correlation between stereotactic radiosurgery treatments and αv subunit, αvβ3, αvβ6, αvβ8 or β3 subunit expression was observed. Prior WBRT or chemotherapy did not show a significant correlation with expression of any of the integrin subunits investigated in this study.

Cadherin expression

42/57 (73.7%) tumor specimens showed expression of E cadherin, 10/57 (17.5%) of N cadherin and 6/57 (10.5%) showed expression of both cadherins. No significant correlation of median H-score of E cadherin or N cadherin and invasion pattern or primary tumor types was observed. 9/57 (15.8%) specimens showed increased E cadherin expression at the invasion front. 3/57 (5.3%) specimens showed overlapping increased expression at the invasion front of E cadherin and αv, 2/57 (3.5%) overlapping expression with αvβ5 and 1/57 (1.8%) specimen overlapping expression with αvβ6 at the invasion front. No cadherin expression was observed in the tumor stroma or vascular structures.

DISCUSSION

Brain metastases are an increasing challenge in oncological practice, as survival in many types of solid cancers is increased by novel treatment strategies. The dominant treatment strategies for brain metastases are local and include surgery and radiosurgery. The benefit from local treatments is likely to be heavily impacted by the degree to which macroscopically focal disease is truly focal on a microscopic level. Accordingly, the brain metastasis/brain interface may assume major prognostic significance.

Here, we delineate three distinct invasion patterns of brain metastases: well-demarcated growth, vascular co-option and diffuse infiltration. We found a high fraction of cases showing invasive growth via vascular co-option (18%) or single cell infiltration (32%). These surprising findings challenge the general notion that brain metastases predominantly grow in an expansive and well-delineated fashion, but are in good agreement with previous results from experimental studies, smaller and less comprehensive investigations on human tissue samples, and from clinical observations.

In half of our cases, we observed expansive growth of an outwardly extending tumor mass within the brain parenchyma. αvβ6 expression levels were significantly higher in this group of well-demarcated tumors. Integrin αvβ6 is not expressed in healthy adult epithelia but is up-regulated in cancer and has been shown to modulate invasion and inhibit apoptosis.[23] However, the exact role of αvβ6 in cancer pathobiology and in particular in brain metastases remains to be determined.

The vascular basement membrane may act as guiding track for perivascular growth of cell collectives. Our results indicate that this invasion behavior is present not only in mesenchymal and epithelial tissues, but also occurs in the distinct microenvironment of the CNS. In line with previous studies we observed vascular co-option most commonly in melanoma brain metastases, however, we found it also in other tumor types such as NSCLC adenocarcinoma. [24-26]

Single cell infiltration into the brain parenchyma of brain-metastatic tumor cells has previously been reported to be characteristic for SCLC. [7] Our data show that this invasion patterns is not uncommon also in brain metastases of other tumor types including NSCLC adenocarcinoma/ squamous cell carcinoma, breast cancer and melanoma. The high fraction of brain metastases cases showing infiltrative growth has implications for local therapy options and highlights the need for including a safety margin beyond the neuroradiologically visible tumor borders.[6] In our study, depth of invasion into the CNS parenchyma from the main tumor mass reached up to 450 µm. Of note, stereotactic radiosurgery uses no margins for treatment, but at 0.4 mm from the prescription isodose line near full dose is delivered, and therefore, the magnitude of invasion has no clear consequence on stereotactic radiosurgery practice. The selection of patients in need for an extended local treatment approach is challenging as the current neuro-radiological techniques cannot precisely visualize the invasion distance of a given tumor. However, we previously demonstrated that the extent of peritumoral brain edema might function as a surrogate marker for infiltrative tumor growth, as little brain edema was significantly more common in infiltrative brain metastases and correlated with impaired patient survival times. [8]

Further prospective studies need to address the prognostic implications of brain metastases invasion patterns in more detail.

We did not observe a statistically significant correlation of treatment modality with invasion pattern in our cohort. However, a higher proportion of patients in the diffuse infiltration group had received prior radiation or chemotherapy.. As our sample size is not adequate for firm statistical conclusions, we cannot exclude that radio- or chemotherapy may select for or produce tumor cell with a higher infiltrative potential, similarly to some observations in primary tumors and gliomas. [27] Interestingly, brain metastases lesions previously treated with stereotactic radiotherapy showed higher expression of αvβ5, a finding which is well in line with previous reports showing that this molecule is essential for tumor growth in preirradiated stroma. [28] Further, we observed a high consistency of invasion behavior between the growth patterns of different brain metastases in individual patients. This again may indicate that intrinsic molecular features of metastases originating from a given primary tumor correlate with certain invasion patterns.

Our results have to interpreted with caution since the small sample sizes often do not allow firm statistically conclusions. Herein, we concentrated on the descriptive presentation of our results. However, it has to be taken into account that autopsy samples of BRAIN METASTASES are very rare and our series displays a rather large cohort compared to previously published studies on autopsy specimens. [6,7]

We noted prominent expression of αv integrins in many brain metastases cases. This underscores the important function of this class of molecules in metastatic

cancer. Currently, several integrin inhibitors are under clinical development and promising activity was shown in some of the most frequent primary tumors of brain metastases such as NSCLC and melanoma. [29-31] Interestingly, the anti-αv-integrin antibody intetumumab reduced brain metastases outgrowth in mice after intra-carotid infusion of brain-seeking HER2-postive breast cancer cells. [32] Thus, clinical trials specifically investigating the potential of integrin inhibitors for prophylaxis and treatment of brain metastases seem warranted.

ACKNOWLEDGMENT

We thank Irene Leisser and Gerda Ricken for excellent technical assistance with preparation of tissue specimens. Further we thank Prof. Dr. Harald Heinzl (Center for Medical Statistics, Informatics, and Intelligent Systems, Medical University of Vienna) for the supervision and advice with statistical analyses. This study was performed within the PhD thesis project of Anna Sophie Berghoff in the PhD program “Clinical Neuroscience (CLINS)” at the Medical University Vienna.

REFERENCES

1. Gavrilovic IT, Posner JB. Brain metastases: epidemiology and pathophysiology. *J Neurooncol.* Oct 2005;75(1):5-14.

2. Gaspar LE, Mehta MP, Patchell RA, et al. The role of whole brain radiation therapy in the management of newly diagnosed brain metastases: a systematic review and evidence-based clinical practice guideline. *J Neurooncol.* Jan 2010;96(1):17-32.

3. Kalkanis SN, Kondziolka D, Gaspar LE, et al. The role of surgical resection in the management of newly diagnosed brain metastases: a systematic review and evidence-based clinical practice guideline. *J Neurooncol.* Jan 2010;96(1):33-43.

4. Linskey ME, Andrews DW, Asher AL, et al. The role of stereotactic radiosurgery in the management of patients with newly diagnosed brain metastases: a systematic review and evidence-based clinical practice guideline. *J Neurooncol.* Jan 2010;96(1):45-68.

5. Wesseling P, von Deimling A, Aldape K. *Metastatic tumours of the CNS*. 4th ed. Lyons, France: IARC Press; 2007.

6. Baumert BG, Rutten I, Dehing-Oberije C, et al. A pathology-based substrate for target definition in radiosurgery of brain metastases. *Int J Radiat Oncol Biol Phys.* Sep 1 2006;66(1):187-194.

7. Neves S, Mazal PR, Wanschitz J, et al. Pseudogliomatous growth pattern of anaplastic small cell carcinomas metastatic to the brain. *Clin Neuropathol.* Jan-Feb 2001;20(1):38-42.

8. Spanberger T, Berghoff AS, Dinhof C, et al. Extent of peritumoral brain edema correlates with prognosis, tumoral growth pattern, HIF1a expression and angiogenic activity in patients with single brain metastases. *Clin Exp Metastasis.* Oct 17 2012.

9. McPherson CM, Suki D, Feiz-Erfan I, et al. Adjuvant whole-brain radiation therapy after surgical resection of single brain metastases. *Neuro Oncol.* Jul 2010;12(7):711-719.

10. Friedl P, Alexander S. Cancer invasion and the microenvironment: plasticity and reciprocity. *Cell.* Nov 23 2011;147(5):992-1009.

11. Desgrosellier JS, Cheresh DA. Integrins in cancer: biological implications and therapeutic opportunities. *Nat Rev Cancer.* Jan 2010;10(1):9-22.

12. Guo W, Giancotti FG. Integrin signalling during tumour progression. *Nat Rev Mol Cell Biol.* Oct 2004;5(10):816-826.

13. Hood JD, Cheresh DA. Role of integrins in cell invasion and migration. *Nat Rev Cancer.* Feb 2002;2(2):91-100.

14. Bonneh-Barkay D, Wiley CA. Brain extracellular matrix in neurodegeneration. *Brain Pathol.* Oct 2009;19(4):573-585.

15. Mazal PR, Czech T, Sedivy R, et al. Prognostic relevance of intracytoplasmic cytokeratin pattern, hormone expression profile, and cell proliferation in pituitary adenomas of akromegalic patients. *Clin Neuropathol.* Jul-Aug 2001;20(4):163-171.

16. Gelpi E, Popovic M, Preusser M, Budka H, Hainfellner J. Pleomorphic xanthoastrocytoma with anaplastic features presenting without GFAP immunoreactivity: implications for differential diagnosis. *Neuropathology.* Sep 2005;25(3):241-246.

17. Birner P, Piribauer M, Fischer I, et al. Vascular patterns in glioblastoma influence clinical outcome and associate with variable expression of angiogenic proteins: evidence for distinct angiogenic subtypes. *Brain Pathol.* Apr 2003;13(2):133-143.

18. Goodman SL, Grote HJ, Wilm C. Matched rabbit monoclonal antibodies against alphav-series integrins reveal a novel alphavbeta3-LIBS epitope, and permit routine staining of archival paraffin samples of human tumors. *Biol Open.* Apr 15 2012;1(4):329-340.

19. Schittenhelm J, Schwab EI, Sperveslage J, et al. Longitudinal Expression Analysis of alphav Integrins in Human Gliomas Reveals Upregulation of Integrin alphavbeta3 as a Negative Prognostic Factor. *J Neuropathol Exp Neurol.* Mar 2013;72(3):194-210.

20. Cappuzzo F, Hirsch FR, Rossi E, et al. Epidermal growth factor receptor gene and protein and gefitinib sensitivity in non-small-cell lung cancer. *J Natl Cancer Inst.* May 4 2005;97(9):643-655.

21. Hirsch FR, Varella-Garcia M, Bunn PA, Jr., et al. Epidermal growth factor receptor in non-small-cell lung carcinomas: correlation between gene copy number and protein expression and impact on prognosis. *J Clin Oncol.* Oct 15 2003;21(20):3798-3807.

22. Bender R, Lange S. Adjusting for multiple testing--when and how? *J Clin Epidemiol.* Apr 2001;54(4):343-349.

23. Bandyopadhyay A, Raghavan S. Defining the role of integrin alphavbeta6 in cancer. *Curr Drug Targets.* Jul 2009;10(7):645-652.

24. Kienast Y, von Baumgarten L, Fuhrmann M, et al. Real-time imaging reveals the single steps of brain metastasis formation. *Nat Med.* Jan 2010;16(1):116-122.

25. Dome B, Paku S, Somlai B, Timar J. Vascularization of cutaneous melanoma involves vessel co-option and has clinical significance. *J Pathol.* Jul 2002;197(3):355-362.

26. Leenders WP, Kusters B, Verrijp K, et al. Antiangiogenic therapy of cerebral melanoma metastases results in sustained tumor progression via vessel co-option. *Clin Cancer Res.* Sep 15 2004;10(18 Pt 1):6222-6230.

27. Wild-Bode C, Weller M, Rimner A, Dichgans J, Wick W. Sublethal irradiation promotes migration and invasiveness of glioma cells: implications for radiotherapy of human glioblastoma. *Cancer Res.* Mar 15 2001;61(6):2744-2750.

28. Monnier Y, Farmer P, Bieler G, et al. CYR61 and alphaVbeta5 integrin cooperate to promote invasion and metastasis of tumors growing in preirradiated stroma. *Cancer Res.* Sep 15 2008;68(18):7323-7331.

29. Goodman SL, Picard M. Integrins as therapeutic targets. *Trends Pharmacol Sci.* Jul 2012;33(7):405-412.

30. Manegold C, Vansteenkiste J, Cardenal F, et al. Randomized phase II study of three doses of the integrin inhibitor cilengitide versus docetaxel as second-line treatment for patients with advanced non-small-cell lung cancer. *Invest New Drugs.* Feb 2013;31(1):175-182.

31. O'Day S, Pavlick A, Loquai C, et al. A randomised, phase II study of intetumumab, an anti-alphav-integrin mAb, alone and with dacarbazine in stage IV melanoma. *Br J Cancer.* Jul 26 2011;105(3):346-352.

32. Wu YJ, Muldoon LL, Gahramanov S, Kraemer DF, Marshall DJ, Neuwelt EA. Targeting alphaV-integrins decreased metastasis and increased survival in a nude rat breast cancer brain metastasis model. *J Neurooncol.* Oct 2012;110(1):27-36.

FIGURE LEGENDS

Figure 1: Distinct invasion patterns in human brain metastases. A example of well-demarcated invasion (Patient 5, NSCLC, supplemental Table 1): Aa H&E slide (magnification X 1.25); Ab: Invasion front of well-demarcated brain metastasis (magnification x 400); Ac: Macroscopic sample of well-demarcated brain metastasis; Ad MRI contrast-enhanced T1-weighted sequence sample of well-demarcated brain metastasis; B example of vascular co-option (Patient 13, melanoma, supplemental Table 1): Ba: H&E slide (magnification x 1.25); Bb: CD34 immunohistochemistry of vascular co-option (magnification X 400); Bc: Macroscopic sample of brain metastasis growing via vascular co-option; Bd MRI contrast-enhanced T1-weighted sequence sample of brain metastasis growing via vascular co-option; C example of diffuse invasion (Patient 2, SCLC, supplemental Table 1); Ca H&E of brain metastasis (magnification x 1.25); Cb: CD18 cytokeratin staining showing diffusely infiltrating tumor cells; Cc: Macroscopic sample of diffuse infiltrating brain metastasis; Cd MRI contrast-enhanced T1-weighted sequence sample of diffuse infiltrating brain metastasis.

Figure 2: Integrin expression patters: A: αv subunit expression (Patient 5, NSCLC, supplemental Table 1); B: αvβ5 expression with accentuation around a vessel (Patient 5, NSCLC, supplemental Table 1); C: αvβ5 expression in a brain metastasis growing via vascular co-option (Patient 13, melanoma, supplemental Table 1); D αvβ6 expression with accentuation around necrosis, star marks necrosis (Patient 5, NSCLC, supplemental Table 1).

Figure 3: Integrin expression in vascular structures. A: αvβ3 expression on tumor vessel, arrow marks a vessel in the peritumoral area without αvβ3 expression

(Patient 5, NSCLC, supplemental Table 1), B: αvβ3 expression in glomeruloid-like vessels of the peritumoral area, star marks the tumor tissue, the cross marks the surrounding cerebellum (Patient 8, SCLC, supplemental Table 1), C: αvβ3 expression in a vessel with vascular co-option Patient 13, melanoma, supplemental Table 1), D: CD34 immunohistochemistry of the case shown in B, illustrating the peritumoral sprouting vessels (Patient 8, SCLC, supplemental Table 1).

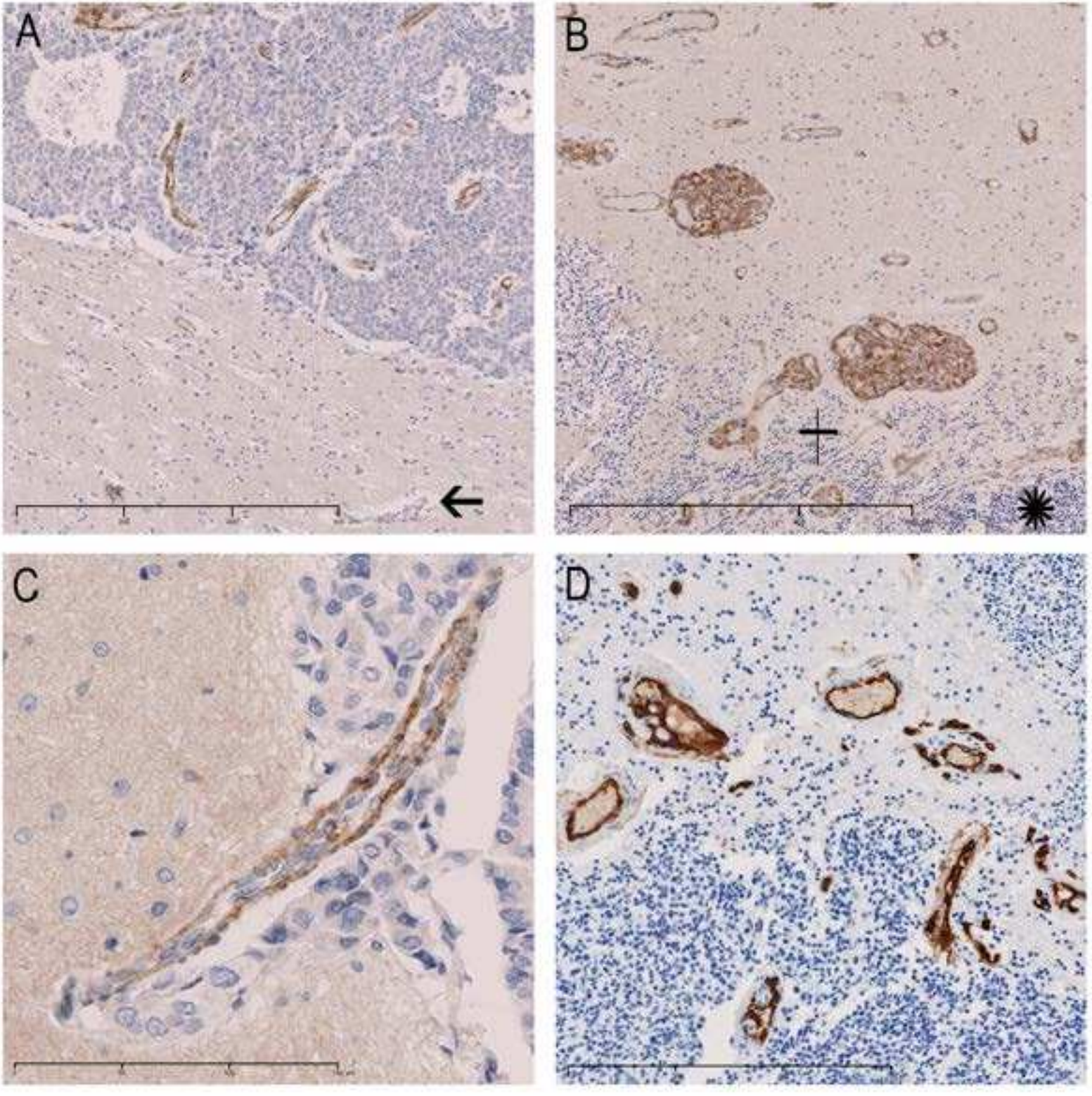
A
B
C
D

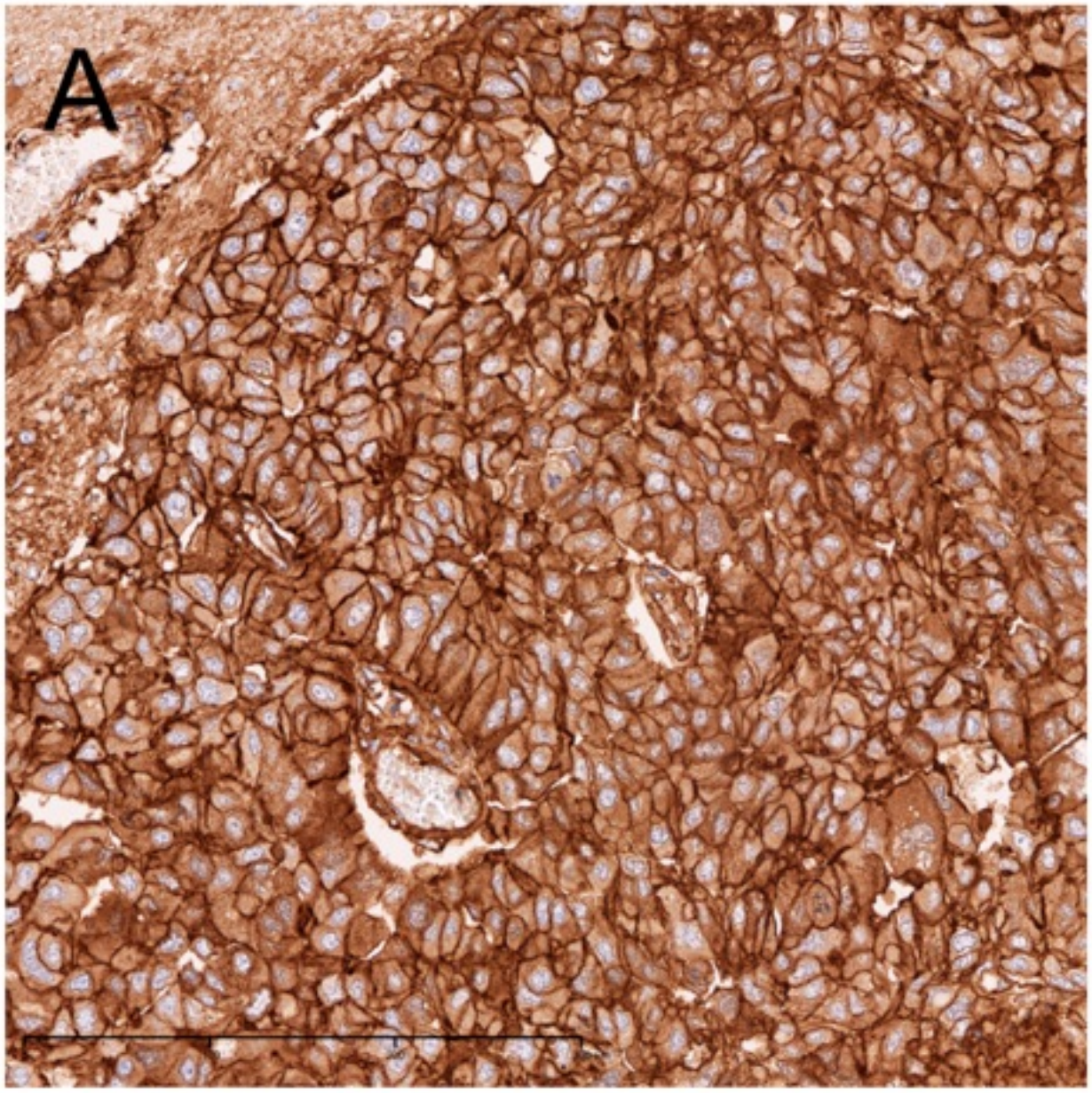
A

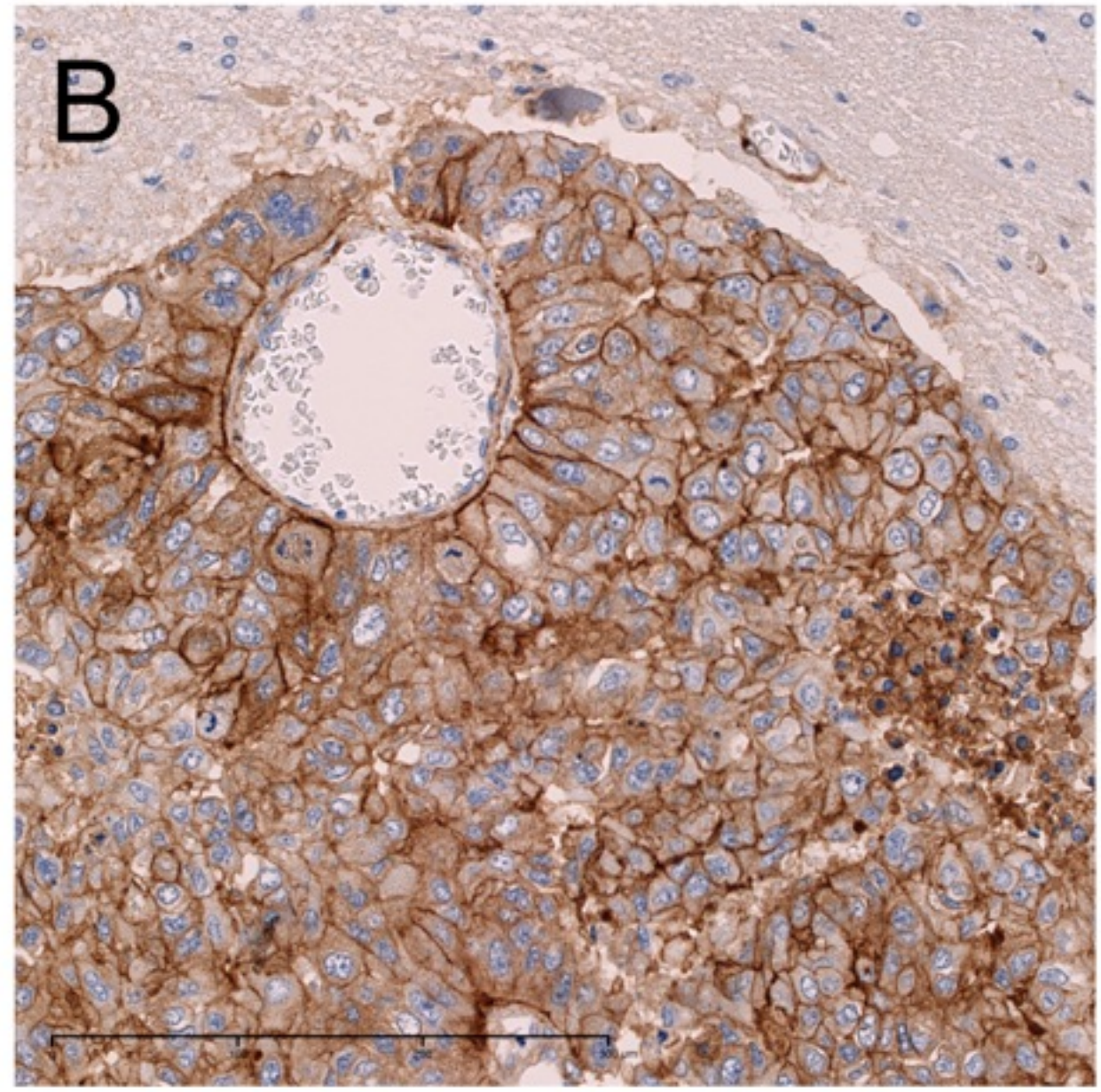
B

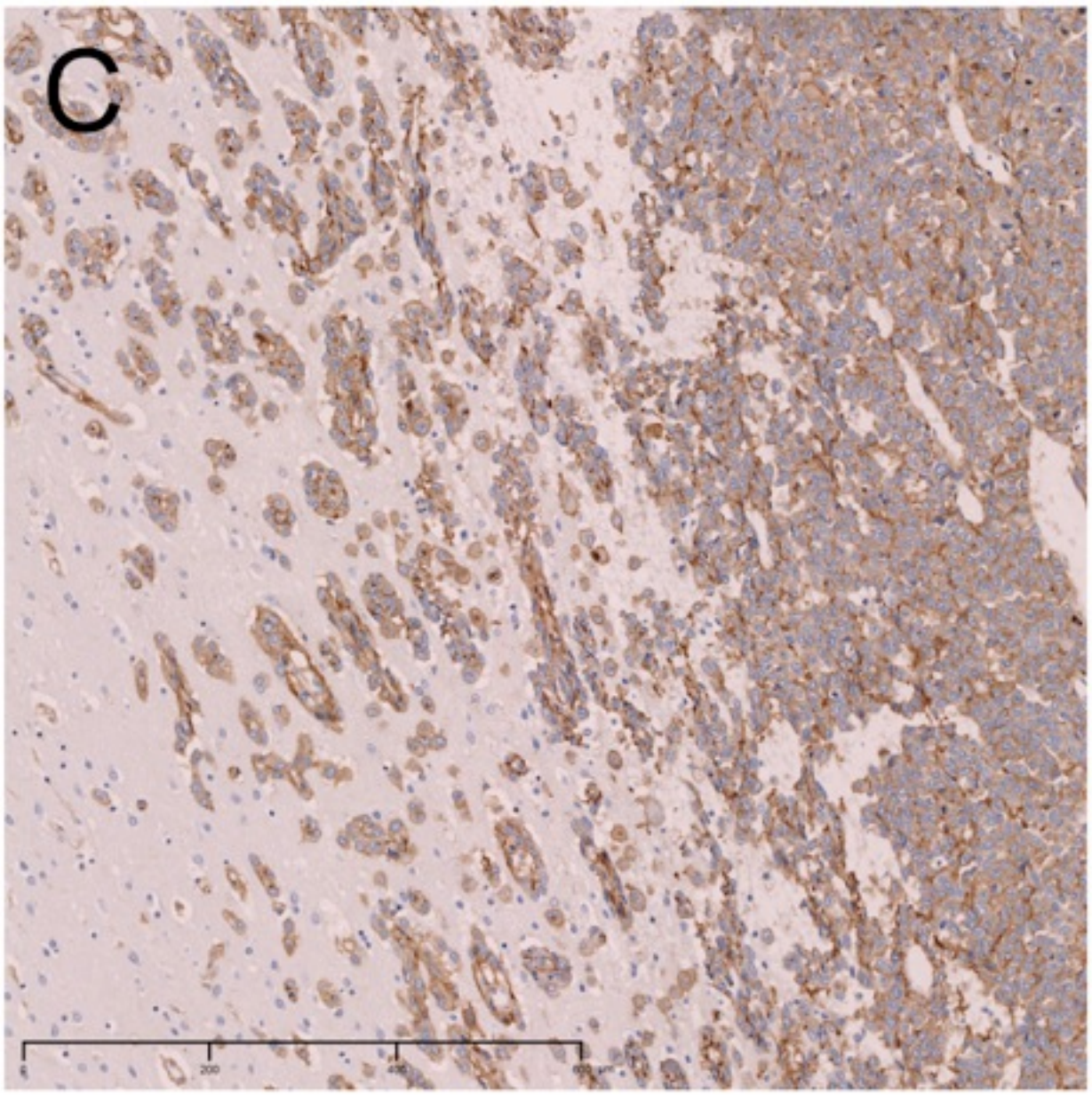
C

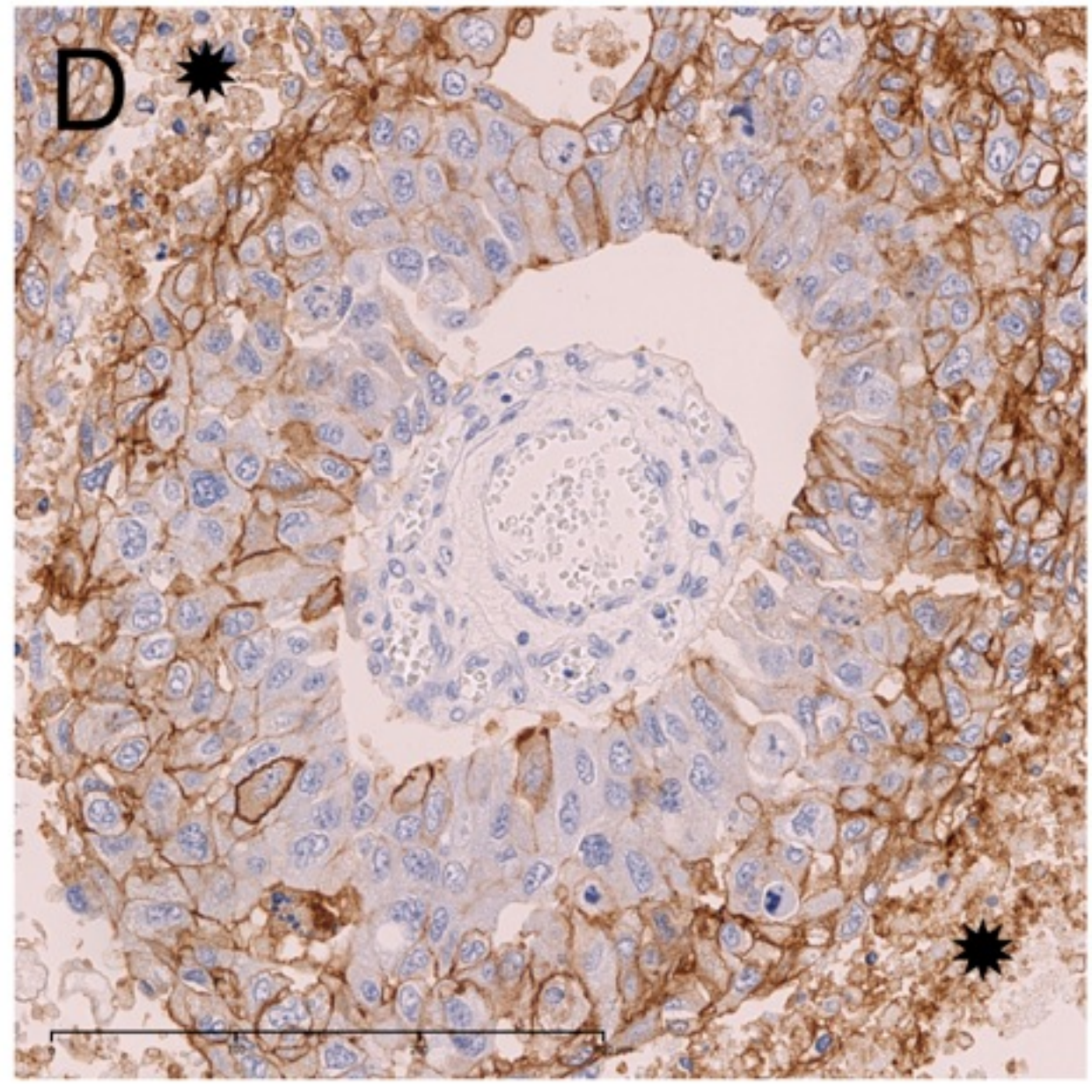
D

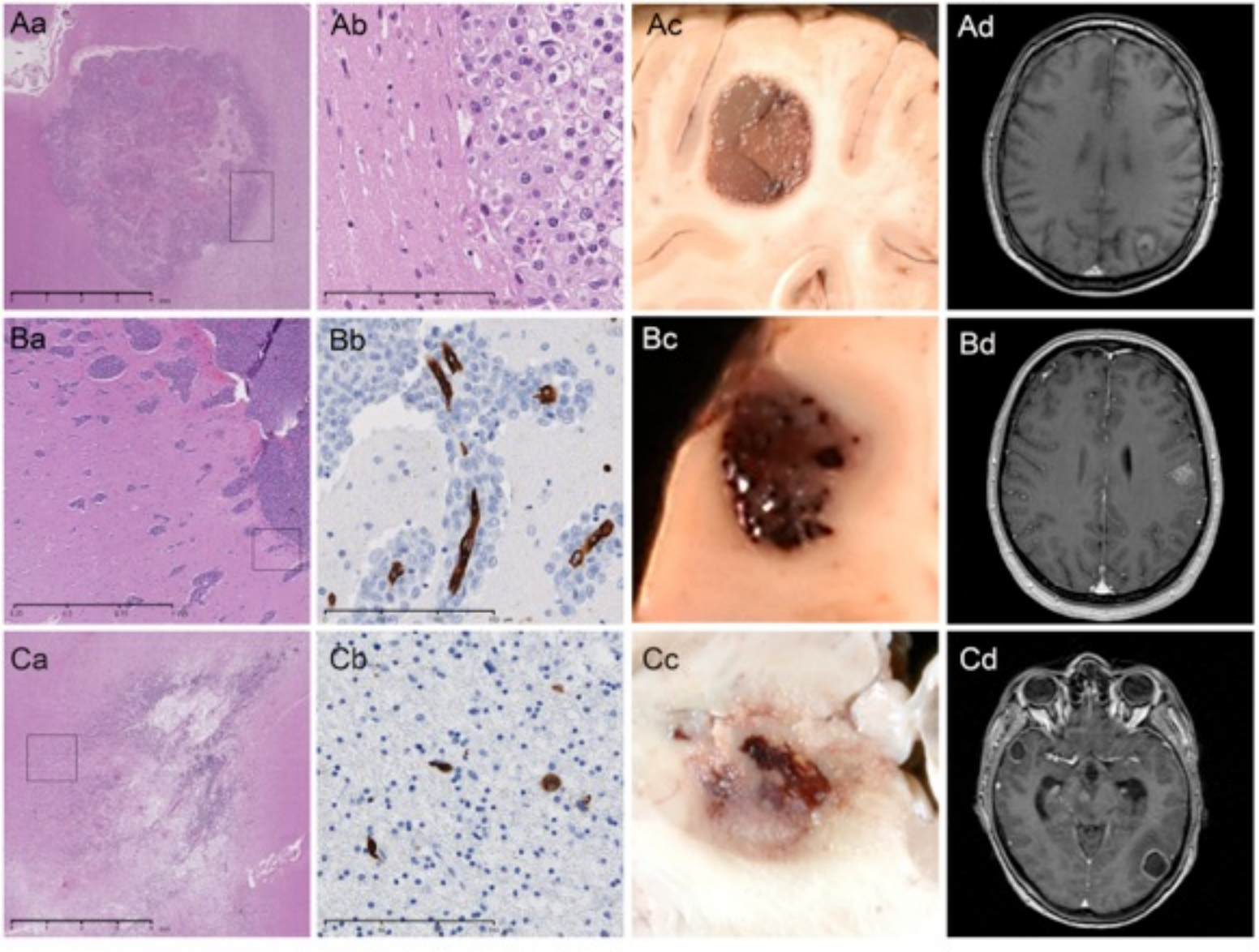
Aa
Ab
Ac
Ad
Ba
Bb
Bc
Bd
Ca
Cb
Cc
Cd